DOI: 10.61782/fa.2023.1004

forum acusticum 2023

INFLUENCE OF MANUFACTURING TECHNOLOGY ON THE ACOUSTIC PERFORMANCE OF METAMATERIALS

Elio Di Giulio[1*] **Marialuisa Napolitano**[1] **Rosario Aniello Romano**[1]
Antonio Scofano[2] **Raffaele Dragonetti**[1]
[1]Industrial Engineering Department, University of Naples *Federico II*, Italy.
[2] Z Lab S.R.L.,Verona, Italy.

ABSTRACT

The potential of the manufacturing technologies, such as Selective Laser Melting (SLM) and Digital Light Processing (DLP), has made it feasible today to realize particular structures in a variety of materials and geometrical dimensions, that were unattainable using conventional production methods. Nevertheless, several features of the manufacturing technology assume a fundamental role on the acoustic response of the realized material. In this work, the influence of the manufacturing processes in the realization of acoustic metamaterial with extended surfaces has been investigated. The acoustic behaviour of the metamaterial is analytically described by using the Transfer Matrix Method (TMM), while numerical modelling is performed with a Finite Element software (FEM). Experimental investigations have been carried out on different samples of the designed metamaterial made by 3D-printing and Laser technology on behalf of the Company Z Lab (Cerea, VR). Each sample has been made with different features and surface finish. The experimental results are reported in terms of the sound absorption coefficient at normal incidence and Transmission Loss.

Keywords: *Metamaterial, manufacturing process, sound absorption.*

**Corresponding author*: *elio.digiulio@unina.it.*

1. INTRODUCTION

Acoustic metamaterials are a relatively new class of materials that have the potential to revolutionize the field of acoustics. These materials are engineered to have unique properties that allow them to manipulate sound waves in ways that were previously impossible. By controlling the propagation of sound, acoustic metamaterials have the potential to improve the performance of a wide range of acoustic devices, from loudspeakers and microphones to noise barriers and medical imaging equipment [1, 2] One of the key properties of acoustic metamaterials is their ability to bend and control the path of sound waves. This is achieved by designing the material's internal structure to have a specific pattern of repeating elements that can redirect and scatter sound waves in precise ways. Another important property is the ability to create negative acoustic properties, such as negative density or negative modulus, which can lead to interesting effects like acoustic cloaking and subwavelength imaging [3]. While the field of acoustic metamaterials is still relatively new, researchers are already exploring a wide range of potential applications, including noise reduction in buildings and transportation, improved acoustic imaging for medical diagnostics, and even new types of musical instruments. As the field continues to develop, it is likely that we will see even more exciting and innovative uses for these fascinating materials. Acoustic metamaterials can be broadly classified into two categories: locally resonant metamaterials and membrane metamaterials. Locally resonant metamaterials are designed to have internal structures that resonate at specific frequencies, allowing them to filter out unwanted frequencies and manipulate sound waves in various ways. Membrane metamaterials, on the other hand,

are thin sheets with periodic structures that can block or allow the transmission of sound waves, depending on the size and spacing of the structures. Within these two categories, there are many different designs and variations of acoustic metamaterials, each with unique properties and potential applications [4]. The aim of this research is to investigate on the effect of the manufacturing processes, such as the 3D printing and the Digital Laser Processing, on the performances of acoustic metamaterials. Two different Helmholtz Resonator based metamaterial have been realized using these techniques, presented in the Sec. 2. Sec. 3 presents the formulation to analytically model the metamaterial. Subsequently, experimental results are reported in Sec. 4 and compared with the theoretical trends. Sec. 5 concludes the work with future remarks.

2. MANUFACTURING PROCESSES

3D printing and laser machining have revolutionized the field of acoustic metamaterials, enabling researchers to create complex and intricate structures that were once impossible to produce. 3D printing allows for the fabrication of structures with high geometrical complexity, including those with features on the scale of micrometers. This technique is particularly useful for creating customized metamaterial structures that are tailored to specific applications, such as acoustic lenses or cloaks. In addition, 3D printing can produce metamaterials with tunable properties, such as the stiffness and density of the printed material. Laser machining, on the other hand, allows for the creation of precise patterns on the surface of a material, enabling the production of acoustic metamaterials with sub-wavelength features. This technique can produce metamaterials with high resolution and in a variety of materials, including metals, polymers, and composites. Laser machining can be used to create acoustic metamaterials with specific geometries and properties, such as negative refractive index or perfect absorption. Both 3D printing and laser machining have their strengths and weaknesses when it comes to fabricating acoustic metamaterials [5]. For example, 3D printing is better suited for producing larger structures with lower resolution, while laser machining is better suited for producing smaller structures with higher resolution. Nonetheless, these techniques are highly complementary, and researchers often use a combination of 3D printing and laser machining to create acoustic metamaterials with the desired properties and capabilities. The first sample, referred to as 3D-printed metamaterial, is realized through a nozzle which realizes the material by successive deposition of layers, Fig. 1. On the right side of Fig. 1, it can be noticed how visible is this process on the final sample. In particular, the roughness could not always have a negligible effect, especially where the size are very small, i.e. the neck of the Helmholtz Resonator. The second designed metamaterial is realized with Digital Light Processing machine which uses a projected light source to cure the entire layer at once. The overall effect is greater accuracy in detail, as it can be seen in Fig. 2.

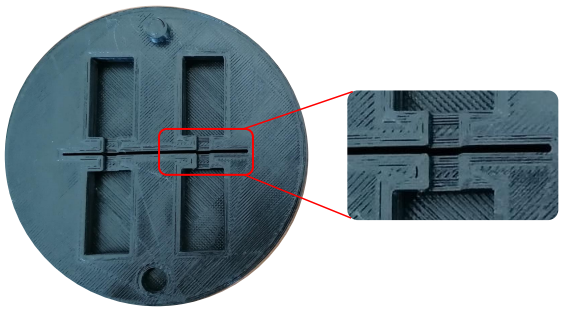

Figure 1. On the left, one side of the 3D-printed Metamaterial. On the right, a detail on the layers deposited during the manufacturing process is reported.

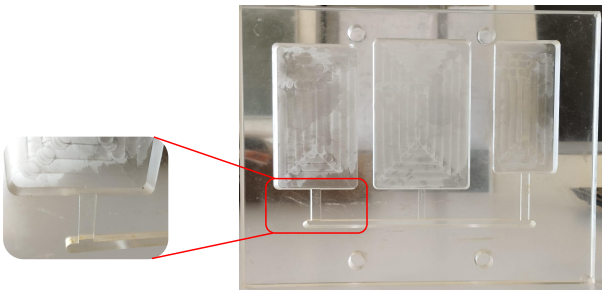

Figure 2. On the right, one side of the Metamaterial sample made through Digital Light Processing. On the left, a detail of the superficial roughness.

3. TRANSFER MATRIX METHOD

The Transfer Matrix approach is a powerful mathematical tool to link the state variables, such as the acoustic pres-

sure and volume velocity, between two side of a certain material, where d and A are respectively the thickness and the cross sectional area,

$$\begin{bmatrix} p_1 \\ U_1 \end{bmatrix}_{x=d} = \begin{bmatrix} \cos(\tilde{k}d) & i\frac{\tilde{Z}}{A}\sin(\tilde{k}d) \\ i\frac{A}{\tilde{Z}}\sin(\tilde{k}d) & \cos(\tilde{k}d) \end{bmatrix} \begin{bmatrix} p_1 \\ U_1 \end{bmatrix}_{x=0}. \quad (1)$$

$\tilde{Z}$ and $\tilde{k}$ are the characteristic impedance and complex wavenumber of the material. The quantities are linked to the viscous and thermal characterization of each geometry-material from the relations, said $\omega = 2\pi f$ the angular frequency,

$$\tilde{k} = \omega\sqrt{\frac{\tilde{\rho}}{\tilde{K}}}, \quad (2)$$

$$\tilde{Z} = \sqrt{\tilde{\rho}\tilde{K}}, \quad (3)$$

where $\tilde{\rho}$ and $\tilde{K}$ are the complex and frequency-dependent density and bulk modulus of the material. For the designed geometries these two quantities are characterized by analytical expressions reported in the next subsection.

3.1 Metamaterial modeling

The designed Metamaterial geometries consist of a slit whose is loaded on by two Helmholtz resonators with square neck and cavity, as shown in Fig. . The first sample is characterized by four identical Helmholtz Resonators (HR) which are parallel-assembled on the slit with respect to the sound wave, Fig. 1. The second specimen is made by three different HRs, always loaded in parallel on the slit. The slit is a fundamental element in the acoustic performance of the system as it allows to realize, within it, the conditions of so-called slow sound, lowering resonance frequency of the Helmholtz resonator and improving its performance at low frequencies, with the same overall dimensions of the resonator itself, thus optimizing the available space. It is in fact worth noting that the speed of sound within a slit is lower than that of sound in free air.

3.1.1 Slit

Effective parameters of the slit are expressed as

$$\tilde{\rho}_s = \rho_0\left[1 - \frac{\tanh\left(\frac{h_s}{2}G_\nu\right)}{\frac{h_s}{2}G_\nu}\right], \quad (4)$$

$$\tilde{K}_s = \gamma p_0\left[1 + (\gamma-1)\frac{\tanh\left(\frac{h_s}{2}G_\kappa\right)}{\frac{h_s}{2}G_\kappa}\right]. \quad (5)$$

Here, $G_\nu = \sqrt{i\omega\rho_0/\mu}$ and$G_\kappa = \sqrt{i\omega P_r\rho_0/\mu}$, where ρ_0, p_0, γ, μ and P_r are respectively the static density, the ambient pressure, the heat capacity ratio, the dynamic viscosity and the Prandtl number of the air.

3.1.2 Helmholtz Resonator: neck and cavity

The neck and cavity of the HR are characterized by squared shapes, and the complex density and bulk modulus can be expressed as

$$\tilde{\rho}_{n(c)} = -\rho_0\frac{a^2b^2}{4G_\nu^2\sum_{k\in\mathbb{N}}\sum_{m\in\mathbb{N}}[\alpha_k^2\beta_m^2(\alpha_k^2+\beta_m^2-G_\nu^2)]^{-1}}, \quad (6)$$

$$\tilde{K}_{n(c)} = \frac{\gamma p_0}{\gamma + \frac{4(\gamma-1)G_\kappa^2}{a^2b^2}\sum_{k\in\mathbb{N}}\sum_{m\in\mathbb{N}}[\alpha_k^2\beta_m^2(\alpha_k^2+\beta_m^2-G_\kappa^2)]^{-1}}, \quad (7)$$

where $\alpha_k = \frac{2(k+\frac{1}{2})\pi}{a}$, $\beta_m = \frac{2(m+\frac{1}{2})\pi}{b}$, a and b are the sides lengths of the ducts cross-section (for square ducts, they are identical and equal to l_n and l_c , respectively for neck and cavity).

3.1.3 Metamaterial

The analytical modeling of the considered metamaterials can be obtained from the overall transfer matrix of the system

$$\mathbf{T_t} = \mathbf{T_{rad}}\mathbf{T_{slit}}\mathbf{T}_{//,\mathbf{HR}}\mathbf{T_{slit}}. \quad (8)$$

Transfer matrix for each of the two identical slit portions, $\mathbf{T_{slit}}$, is written as

$$\mathbf{T_{slit}} = \begin{bmatrix} \cos(\tilde{k}_s\frac{b_s}{2}) & i\frac{\tilde{Z}_s}{A_s}\sin(\tilde{k}_s\frac{b_s}{2}) \\ i\frac{A_s}{\tilde{Z}_s}\sin(\tilde{k}\frac{b_s}{2}) & \cos(\tilde{k}_s\frac{b_s}{2}) \end{bmatrix}, \quad (9)$$

where $Z_s = \sqrt{\tilde{\rho}_s\tilde{K}_s}$, $\tilde{k}_s = \omega\sqrt{\tilde{\rho}_s/\tilde{K}_s}$. $A_s = a_sh_s$ is the cross-sectional area of the slit, said a_s the width, b_s the depth and h_s the height. The parallel-arranged Helmholtz Resonator is taken into account as

$$\mathbf{T}_{//,\mathbf{HR}} = \begin{bmatrix} 1 & 0 \\ \frac{1}{Z_{HR}} & 1 \end{bmatrix}. \quad (10)$$

Z_{HR} is the ratio between sound pressure and volume velocity at the upstream of each HR, briefly expressed as $Z_{HR} = \mathbf{T_{HR}}(\mathbf{1},\mathbf{1})/\mathbf{T_{HR}}(\mathbf{2},\mathbf{1})$, where $\mathbf{T_{HR}}$ is the

transfer matrix of the Helmholtz Resonator written as

$$\mathbf{T_{HR}} = \begin{bmatrix} \cos(\tilde{k}_n h_n) & i\frac{\tilde{Z}_n}{A_n}\sin(\tilde{k}_n h_n) \\ i\frac{A_n}{\tilde{Z}_n}\sin(\tilde{k}h_n) & \cos(\tilde{k}_n h_n) \end{bmatrix} \times \\ \times \begin{bmatrix} 1 & i\frac{\tilde{Z}_n}{A_n}\tilde{k}_n \Delta l \\ 0 & 1 \end{bmatrix} \begin{bmatrix} \cos(\tilde{k}_c h_c) & i\frac{\tilde{Z}_c}{A_c}\sin(\tilde{k}_c h_c) \\ i\frac{A_c}{\tilde{Z}_c}\sin(\tilde{k}h_c) & \cos(\tilde{k}_c h_c). \end{bmatrix} \tag{11}$$

The subscript n and c indicates the quantities related respectively to the neck and the cavity. Here, the central transfer matrix allows to consider the effects of the pressure radiation at the discontinuity from the neck to the cavity (also from the neck to the slit). The end correction is reported as $\Delta l = \Delta l_1 + \Delta l_2$, where

$$\Delta l_1 = 0.41 \left[1 - 1.35\left(\frac{l_n}{l_c}\right) + 0.31\left(\frac{l_n}{l_c}\right)^3\right] l_n, \tag{12}$$

$$\Delta l_2 = 0.41 \left[1 - 0.235\left(\frac{l_n}{a_s}\right) - 1.32\left(\frac{l_n}{a_s}\right)^2 + \right.$$

$$\left. +1.54\left(\frac{l_n}{a_s}\right)^3 - 0.86\left(\frac{l_n}{a_s}\right)^4\right] l_n. \tag{13}$$

4. EXPERIMENTAL TESTS

The samples have been test under normal incidence waves condition in Kundt's tube. The sound absorption spectra have been experimentally detected from the two microphones' technique, here briefly reported [6].

4.1 Two microphones' technique

The stationary acoustic pressure field in a closed-end tube can be written as

$$p(x) = Ae^{-ikx} + Be^{ikx}, \tag{14}$$

where $k = \omega/c$ is the acoustic wavenumber (c is the sound speed), A and B are respectively the amplitude of the progressive and regressive wave. The complex reflection coefficient is defined as the ration $r = B/A$, as a consequence the sound absorption coefficient is

$$\alpha = 1 - |r|^2. \tag{15}$$

Therefore, in the two microphones' technique, A, B and r can be estimated from the measurement of the acoustic pressure in two point (p_1 and p_2, respectively in x_1 and x_2, as in Fig. 3) as

$$r = \frac{\frac{p_2}{p_1}e^{ik(x_1-x_2)} + 1}{1 - \frac{p_2}{p_1}e^{-ik(x_1-x_2)}} e^{2kx_2}. \tag{16}$$

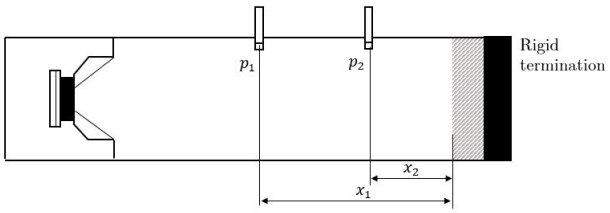

Figure 3. Two microphones' technique scheme.

4.2 Results and discussion

The results are reported in terms of sound absorption coefficient in Figs. 4 and 5 ,respectively for the 3D-printed metamaterial and DLP-based one. The 3D-printed sample is characterized by four identical parallel-assembled HR loaded on a slit. Therefore, $T_{//,HR}(2,1)$ element of the matrix is written as $4/Z_{HR}$, see Eq. 10. The DLP-based metamaterial is made of three different parallel-assembled HRs on a slit and then, three different $T_{//,HR}$ matrices are written taking into account the geometrical features of each HR. The two metamaterial samples are designed to absorb sound energy in different frequency range, in particular resonance phenomena associated to the 3D-printed sample happen around $580\ Hz$, while for the DLP-based sample two sound absorption peak can be detected among $150\ Hz$ and $200\ Hz$ (this is due to the different geometrical dimensions of the HRs).

From these experimental tests, several considerations can be highlighted about the manufacturing technologies for acoustic metamaterials. The goal of such materials is to absorb sound energy (or eventually increase the transmission loss) in a frequency range where classical absorbing system would require geometrical overall dimension which could not meet the design constraints. The energy dissipation mechanism is realized through the interaction of the sound wave with the particular geometrical shapes of the metamaterial. For this reason, very thin channel are often required and the roughness of the surfaces have important weight on the viscous and thermal losses. Therefore, the design process follows the analytical formula-

tions which does not allow to take into account any damping effect due to the not-perfectly smoothed fluid-solid interfaces. This fact is well underlined in Fig. 4, where the experimental results on the 3D-printed metamaterial seem more damped with respect to the analytical prediction. As it can be seen from Fig. 1, the manufacturing technology used for this application leaves geometrical imperfections. The smaller the geometrical dimension to be realized, the greater the influence of the surface roughness (such as the neck of the HR). While, the use of more refined technology such as the Digital Light Processing allow to realize quasi-perfectly smoothed surfaces (Fig. 2), avoiding roughness damping effect as in Fig. 5.

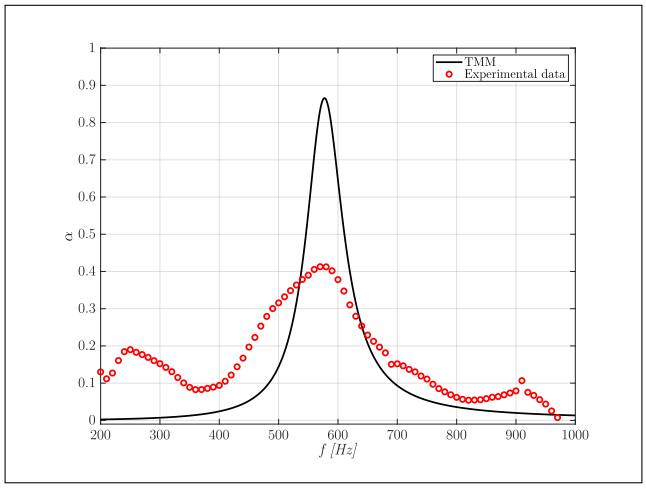

Figure 4. Sound absorption coefficient versus frequency for the 3D-printed Metamaterial sample.

5. CONCLUSION

In this work, a preliminary investigation on the influece of the manufacturing processes on acoustic metamaterials has been presented. Two Helmholtz Resonator based metamaterial have been realized using respectively 3D-printing and Digital Laser Processing techniques. The experimental results have been reported in terms of sound absorption spectrum and compared with the theoretical trends. It is worth to be noticed that the roughness is the most influential parameter. The experimental results on the 3D-printed sample show a greater damped effect due to a lower quality of the surface finishing with respect the results on the DLP sample. By contrast, 3D-printed technology allows specimens to be made in less

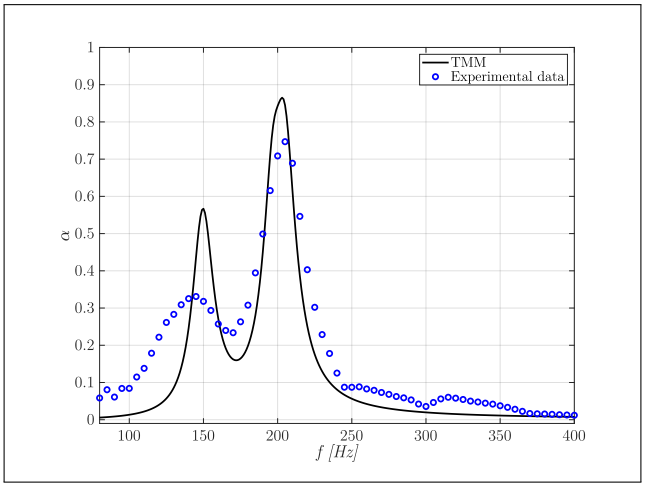

Figure 5. Sound absorption coefficient versus frequency for the SLM-based Metamaterial sample.

time and at a reduced cost compared to DLP technology. Therefore, a trade-off between accuracy of realization and time/cost consuming have to be found based on the design constraints.

6. REFERENCES

[1] S. A. Cummer, J. Christensen, and A. Alù, "Controlling sound with acoustic metamaterials," *Nature Reviews Materials 2016 1:3*, vol. 1, pp. 1–13, feb 2016.

[2] J. Liu, H. Guo, and T. Wang, "A Review of Acoustic Metamaterials and Phononic Crystals," *Crystals 2020, Vol. 10, Page 305*, vol. 10, p. 305, apr 2020.

[3] G. Ma and P. Sheng, "Acoustic metamaterials: From local resonances to broad horizons," *Science Advances*, vol. 2, no. 2, 2016.

[4] "Acoustic Waves in Periodic Structures, Metamaterials, and Porous Media," vol. 143, 2021.

[5] J. Kennedy, L. Flanagan, L. Dowling, G. J. Bennett, H. Rice, and D. Trimble, "The influence of additive manufacturing processes on the performance of a periodic acoustic metamaterial," *International Journal of Polymer Science*, vol. 2019, 2019.

[6] International Organization for Standardization, "ISO 10534-2:1998 - Acoustics — Determination of sound absorption coefficient and impedance in impedance tubes — Part 2: Transfer-function method."